# Electronic structure of $SiO_2$. II. Calculations and results*

Kwok Leung Yip† and W. Beall Fowler
*Department of Physics, Lehigh University, Bethlehem, Pennsylvania 18015*
(Received 4 February 1974)

The techniques developed by the authors have been applied to compute the electronic structure of $SiO_2$ in the $\alpha$-quartz structure by using various clusters of different sizes. The calculated valence-band structure is consistent with the results of other self-consistent-field and semiempirical molecular-orbital calculations, and with the x-ray emission and photoemission data. Among the most interesting results are the following: (i) The width of the valence band is of the order of 9 eV. (ii) The oxygen *sp* hybridization is quite small. (iii) Crossover transitions in a literal sense are negligible. (iv) A residual charge of $-1.2$ on oxygen indicates that the Si-O bond in $SiO_2$ is partly ionic and partly covalent.

## I. INTRODUCTION

This is the second of two papers on the electronic structure of $SiO_2$. In the first paper,[1] we discussed the theory and method involved in the calculation and gave the results of sample calculations on $H_2$ and $H_2O$ molecules. In this paper we present the results for $SiO_2$ and compare them with the results of other calculations and with experimental data.

Recently, extensive experimental studies of the electronic structure of $SiO_2$ have been performed by means of optical,[2-5] x-ray,[6-15] and photoelectron spectroscopy.[16,17] The observed spectra[3,9] for crystalline quartz, fused silica, and $SiO_2$ films grown on Si are found to be very similar to each other, suggesting the importance of short-range order and localized effects in determining the electronic properties of $SiO_2$. In view of the structures[18] of various crystalline and vitreous forms of $SiO_2$, these effects may come from the fundamental existence of the basic $SiO_4$ tetrahedra and their linking $Si_2O$ units. Based on this assumption, most of the published *ab initio*[19,20] and semiempirical[21-27] calculations have used either an $SiO_4$ or an $Si_2O$ cluster as a model representing the solid system. Following the same argument, we shall start our LCLO-MO [(linear combination of localized orbitals)-(molecular orbital)] calculations with the $Si_2O$ and $SiO_4$ clusters. To obtain more reliable information regarding the electronic structure of $SiO_2$, we have extended the calculations to larger clusters such as $Si_2O_7$, $Si_5O_4$, and $Si_8O_7$. For each cluster, the MO results are used to interpret the experimental spectra and are compared with results of other calculations.

## II. ATOMIC CONFIGURATIONS IN $SiO_2$

The atomic positions in $SiO_2$ were obtained from a computer program for right-handed $\alpha$-quartz, in which Smith and Alexander's parameters[28] were used as input data. In Table I, we give the coordinates of 15 atoms which will be included in calculations on different sizes of cluster. The cluster of 15 atoms ($Si_8O_7$) and the coordinate system used are shown in Fig. 1. It is noted that the coordinate system and atomic labelings used here are different from those used by Feigl *et al.*[29]

## III. BASIS FUNCTIONS

Throughout the calculations, the basis functions used are the localized $3s, 3p$ orbitals of silicon and the $2s, 2p$ of oxygen. Although there is a long-standing controversy about the use of Si $3d$ orbitals in MO calculations on $SiO_2$, we have chosen to neglect Si $3d$ orbitals, following Tossell's arguments[27] and the results of Gilbert *et al.*[20] To obtain the localized orbitals (LO's) of silicon and oxygen, we first assume the initial charge configuration of $SiO_2$ to be $Si^{++}(O^-)_2$ which is intermediate between the two suggested extreme cases, namely, very ionic[25] and very covalent.[19,30] In the final stage of our calculation, the Mulliken population analysis[31] will be used to obtain the residual charge on Si and O for a check of self-consistency. Based on this assumption, the localized-orbital equations (in integral form) to be solved are

$$\epsilon_{2s} = K_{2s} + 2F^0(2s,1s) + 2F^0(2s,2s) + 5F^0(2s,2p) - G^0(2s,1s) - G^0(2s,2s) - \tfrac{5}{6}G^1(2s,2p) + V_{2s}, \quad (1)$$

$$\epsilon_{2p} = K_{2p} + 2F^0(2p,1s) + 2F^0(2p,2s) + 5F^0(2p,2p) - \tfrac{6}{25}G^2(2p,2p) + V_{2p} \quad (2)$$

for $O^-$, and

TABLE I. Atomic positions in the right-handed $\alpha$-quartz.[a]

| Atom | Coordinates (in bohr)[b] $x$ | $y$ | $z$ |
|---|---|---|---|
| $Si_0$ | 0.0 | 0.0 | 0.0 |
| $O_I$ | −0.9792 | 2.5854 | −1.2145 |
| $O_{II}$ | 2.7286 | 0.4447 | 1.2145 |
| $O_{III}$ | 0.1514 | −2.1230 | −2.1903 |
| $O_{IV}$ | −1.9143 | −0.9304 | 2.1903 |
| $Si_I$ | −2.7421 | 3.7780 | −3.4048 |
| $Si_{II}$ | 4.6429 | −0.4857 | 3.4048 |
| $Si_{III}$ | 1.9008 | −4.2637 | −3.4048 |
| $Si_{IV}$ | −4.6429 | −0.4857 | 3.4048 |
| $O_V$ | 4.7942 | 1.6374 | 5.5950 |
| $O_{VI}$ | 7.3715 | −0.9304 | 2.1903 |
| $O_{VII}$ | 3.6637 | −3.0711 | 4.6192 |
| $Si_V$ | 6.5437 | 3.3780 | 6.8095 |
| $Si_{VI}$ | 9.2857 | 0.0 | 0.0 |
| $Si_{VII}$ | 1.9008 | −4.2637 | 6.8095 |

[a] Atomic positions are obtained from the $\alpha$-quartz crystal-structure calculation by D. L. Strome (Lehigh University, 1973).

[b] The coordinate system used here is defined in Fig. 1.

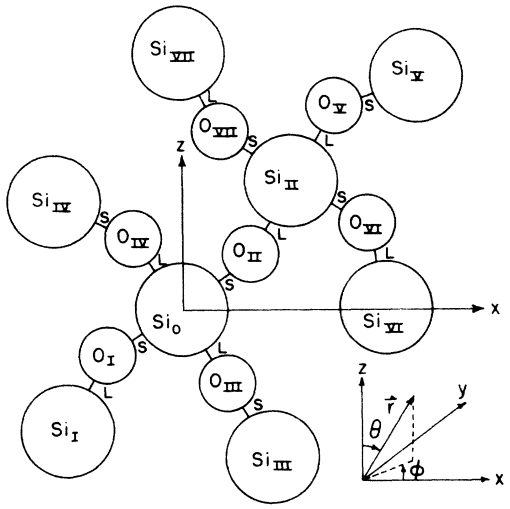


FIG. 1. Atomic configuration in $SiO_2$ (the $Si_8O_7$ cluster). "short" and "long" Si-O bonds are denoted by $S$ and $L$, respectively. ($S = 3.0196\,a_0$, $L = 3.0541\,a_0$). Coordinate system: $x$ is the internuclear axis of $Si_0$ and $Si_{VI}$; $y$ is perpendicular into the page; $z$ is the optic axis, three-fold; and $(\theta, \varphi)$ are polar angles.

$$\epsilon_{3s} = K_{3s} + 2F^0(3s,1s) + 2F^0(3s,2s) + 2F^0(3s,3s) + 6F^0(3s,2p) - G^0(3s,1s) - G^0(3s,2s) - G^0(3s,3s) - G^1(3s,2p) + V_{3s}\,, \tag{3}$$

$$\epsilon_{3p} = K_{3p} + 2F^0(3p,1s) + 2F^0(3p,2s) + F^0(3p,3s) + 6F^0(3p,2p) + F^0(3p,3p) - \tfrac{1}{3}G^1(3p,1s) - \tfrac{1}{3}G^1(3p,2s) - \tfrac{1}{6}G^1(3p,3s) - G^0(3p,2p) - \tfrac{2}{5}G^2(3p,2p) - G^0(3p,3p) + V_{3p} \tag{4}$$

for $Si^{++}$, where $\epsilon_{nl}$, $K_{nl}$, $F^k$, $G^k$, and $V_{nl}$ are all introduced in the previous paper.[1]

In Eqs. (1) and (2) the arbitrary $U_a'$ was chosen as $-U_a$ to form the localizing potential $\rho U_a \rho$, in order to obtain convergent solutions for $O^-$. In constructing the atomic environment potential $U_a$, the detailed part of the potential was calculated only for the nearest and next-nearest neighbors; and the point-ion part of $U_a$ was considered exactly out to about three lattice constants. For simplicity, the system was approximated by an ideal $\beta$-cristobalite structure in calculating the point-ion potential.[32] In Eqs. (1)–(4), only the spherical average part of $U_a$ was used in calculating $V_{nl}$.

In solving Eqs. (1)–(4) we have used the Roothaan analytic expansion method[33] as described in the previous paper. The values of $A_{lj}$ and $Z_{lj}$ for $Si^{++}$ and $O^-$ were obtained from Refs. 34 and 35, respectively. In Tables II and III, we specify

TABLE II. Atomic parameters and energy parameters (in Ry) for $Si^{++}$ in $SiO_2$.

| $j$ | $A_{0j}$ | $Z_{0j}$ | $C_{j30}$ | $A_{1j}$ | $Z_{1j}$ | $C_{j31}$ |
|---|---|---|---|---|---|---|
| 1 | 0 | 15.6334 | 0.18899 | 0 | 10.8139 | 0.00154 |
| 2 | 0 | 12.1835 | −0.34196 | 0 | 6.8493 | 0.06987 |
| 3 | 1 | 11.8216 | 0.19317 | 0 | 4.2336 | 0.09796 |
| 4 | 1 | 7.5755 | −0.40866 | 1 | 3.3949 | 0.01280 |
| 5 | 1 | 5.2061 | 0.73702 | 1 | 1.7195 | −0.13298 |
| 6 | 2 | 4.6712 | −0.28131 | 1 | 1.1824 | −0.93680 |
| 7 | 2 | 2.3810 | 0.20625 | 1 | 0.5932 | 0.06973 |
| 8 | 2 | 1.5647 | −1.10232 | | | |
| 9 | 2 | 0.9866 | −0.05181 | | | |

$\epsilon_{3s} = -2.311469$ $\epsilon_{3p} = -1.821111$
$V_{3s} = 0.927162$ $V_{3p} = 0.780266$
$\epsilon_{3s,3s} = -1.404307$ $\epsilon_{3p,3p} = -1.040845$

TABLE III. Atomic parameters and energy parameters (in Ry) for $O^-$ in $SiO_2$.

| $j$ | $A_{0j}$ | $Z_{0j}$ | $C_{j20}$ | $A_{1j}$ | $Z_{1j}$ | $C_{j21}$ |
|---|---|---|---|---|---|---|
| 1 | 0 | 7.700 | 0.24075 | 0 | 0.714 | 0.05230 |
| 2 | 1 | 1.490 | −0.19862 | 0 | 3.412 | 0.34778 |
| 3 | 1 | 2.803 | −0.43180 | 0 | 1.384 | 0.71241 |
| 4 | 1 | 1.776 | −0.43637 | | | |

$\epsilon_{2s} = -4.727921$ $\epsilon_{2p} = -3.503884$
$V_{2s} = 1.506890$ $V_{2p} = 1.567065$
$\epsilon_{2s,2s} = -3.221031$ $\epsilon_{2p,2p} = -1.936819$

the basis parameters $A_{ij}$ and $Z_{ij}$ used for the $Si^{++}$ and $O^-$ in $SiO_2$ and also give their one-electron eigenvalues $\epsilon_{nl}$ and eigenfunctions $C_{jnl}$ and the expectation values of the atomic environment potential $U_a$ and the Fock operator $F$.

## IV. CALCULATIONS OF THE MATRIX ELEMENTS OF THE FOCK OPERATOR

As specified in the last section, in obtaining the LO's, we actually solved

$$(F_a + U_a + \rho U_a \rho)|ai\rangle = \epsilon_{ai}|ai\rangle \tag{5}$$

for $O^-$, and

$$(F_b + U_b - \rho U_b \rho)|bj\rangle = \epsilon_{bj}|bj\rangle \tag{6}$$

for $Si^{++}$.

From Eqs. (5) and (6), we can write the one-center matrix elements of the Fock operator between LO's as

$$\langle ai|F|aj\rangle = \epsilon_{ai}\delta_{ij} - \langle ai|U_a|aj\rangle \tag{7}$$

for $O^-$, and

$$\langle bi|F|bj\rangle = \epsilon_{bi}\delta_{ij} + \langle bi|U_b|bj\rangle \tag{8}$$

for $Si^{++}$.

Similarly, the two-center matrix elements of the Fock operator can be written as follows:

(i) between $O^-$ and $Si^{++}$,

$$\langle ai|F|bj\rangle = \langle ai|bj\rangle(\epsilon_{ai} + \epsilon_{bj}) - 2\langle ai|U_a|bj\rangle + \langle ai|U_{ab}|bj\rangle - \langle ai|T|bj\rangle\,; \tag{9}$$

(ii) between $Si^{++}$ and $Si^{++}$,

$$\langle ai|F|bj\rangle = \langle ai|bj\rangle(\epsilon_{ai} + \epsilon_{bj}) + \langle ai|U_{ab}|bj\rangle - \langle ai|T|bj\rangle\,; \tag{10}$$

(iii) between $O^-$ and $O^-$,

$$\langle ai|F|bj\rangle = \langle ai|bj\rangle(\epsilon_{ai} + \epsilon_{bj}) - 4\langle ai|U_a|bj\rangle + \langle ai|U_{ab}|bj\rangle - \langle ai|T|bj\rangle\,. \tag{11}$$

To evaluate $\langle ai|U_a|bj\rangle$ and $\langle ai|U_{ab}|bj\rangle$, we expand these matrix elements in powers of the overlap integrals and omit terms of second and higher order in the overlap. We then obtain

$$\langle ai|U_a|bj\rangle \simeq \langle ai|bj\rangle\, U_a(\vec{R}_a)\,, \tag{12}$$

$$\langle ai|U_{ab}|bj\rangle \simeq \langle ai|V_{ab}^{PI} + V_{ab}^{E}|bj\rangle \simeq \langle ai|bj\rangle\, V_b^{PI}(\vec{R}_b) + \langle ai|\frac{Q_a}{\vec{r} - \vec{R}_a}|bj\rangle + \frac{\langle ai|bj\rangle}{|\vec{R}_a - \vec{R}_b|}\,, \tag{13}$$

where $\vec{R}_a$ is the position vector of the $a$th ion with charge $Q_a$, and $V_b^{PI}(\vec{R}_b)$ is the point-ion (PI) potential at the site $b$ which has higher symmetry in the lattice. With approximations (12) and (13), we can calculate the two-center matrix elements of the Fock operator by using Eqs. (9)–(11).

## V. MOLECULAR-ORBITAL STRUCTURE OF THE $Si_2O$ CLUSTER

The nonlinear $Si_2O$ cluster extracted from an $\alpha$-quartz lattice is shown in Fig. 2(a). In Figs. 1 and 2, we show the silicons as approximately twice the size of the oxygens. This is based on the local orbital calculations of the average radii of the valence orbitals of $Si^{++}$ and $O^-$:

$$\langle r\rangle_{Si\,3p} = 2.78 \text{ bohr}, \quad \langle r\rangle_{Si\,3s} = 2.39 \text{ bohr};$$

$$\langle r\rangle_{O\,2p} = 1.48 \text{ bohr}, \quad \langle r\rangle_{O\,2s} = 1.25 \text{ bohr}.$$

An MO energy-level diagram for the nonlinear $Si_2O$ cluster is shown in Fig. 3. MO energies and orbital compositions of filled orbitals are presented in Table IV. Comparisons with other calculations are also given in Table IV.

From our calculations, the oxygen $sp$ hybridization is found negligibly small, in contrast with assumptions made in the semiempirical calculations.[22-24] The electronic configuration for the central oxygen atom is $O^{-1.18}$ ($2s^{1.85}\,2p^{5.33}$), which is fairly consistent with the assumed ionicity for the oxygen atom.

The MO energy-level diagram (Fig. 3) may be used to interpret the O $K\alpha$ soft-x-ray-emission spectrum of $SiO_2$. The assigned transitions are shown in Fig. 3, and the calculated energies and intensities are given in Table V. The calculated

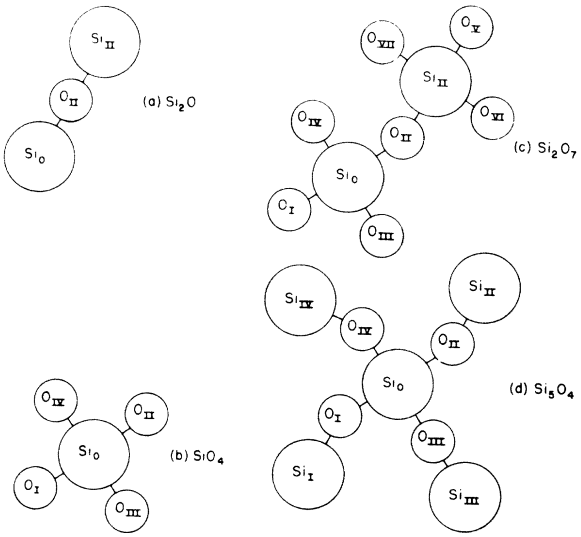


FIG. 2. Schematic clusters extracted from an $\alpha$-quartz lattice.

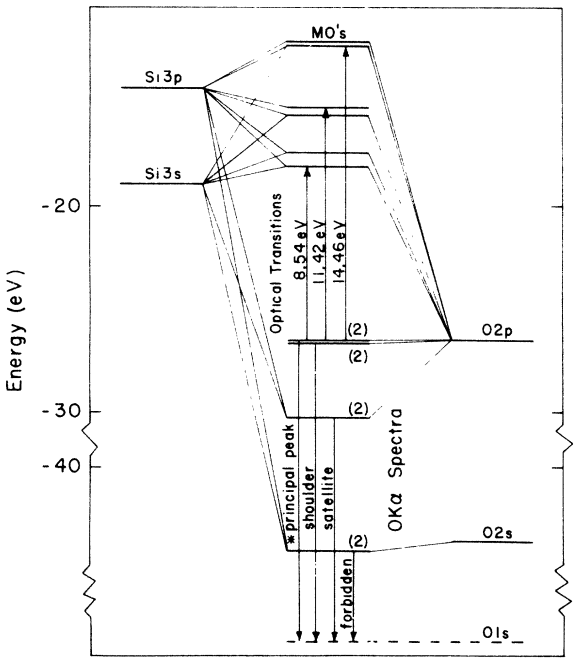


FIG. 3. MO energy-level diagram for nonlinear $Si_2O$ cluster. The number in the parenthesis next to a MO is the occupation number of this orbital.

separation between the principal peak and its satellite, and the calculated position of the principal peak are in reasonable agreement with experimental values. The calculated intensity ratio for the two bands in the O $K\alpha$ spectrum, summed over components, is 3.1/1, which is close to the estimated experimental ratio 4/1 (relative intensities were calculated from the relative O 2$p$ percentage compositions of the related MO's).

From Fig. 3 we can also predict three optical transitions at 8.54, 11.42, and 14.46 eV. These values are in fair agreement with experimental data[3,4,9] (8.3, 11.5, and 14.4 eV). Since the $Si_2O$ cluster is too small to eliminate spurious surface effects, this unusually good agreement is probably fortuitous.

It can be seen from Table IV that the results for a collinear $Si_2O$ calculation are very similar to those of the nonlinear $Si_2O$ calculation. This helps to explain the striking similarities in optical[3] and x-ray[9] spectra between the crystalline and amorphous $SiO_2$, and the importance of short-range order and localized effects in determining the electronic properties of $SiO_2$. It should be noted that we calculate an increase in separation between O $K\alpha$ principal peak and satellite upon bending, whereas Gilbert *et al.*[20] have argued that a decrease should occur. We do not know the cause of this difference.

## VI. MOLECULAR-ORBITAL STRUCTURE OF THE $SiO_4$ CLUSTER

Next, we consider the most basic unit in $SiO_2$, the $SiO_4$ tetrahedron which is shown in Fig. 2(b). Calculations were performed on both the distorted tetrahedral $SiO_4$ cluster in $\alpha$-quartz and the perfect $SiO_4$ tetrahedron in $\beta$-cristobalite. Results are given in Table VI, and compared with *ab initio* and various approximate calculations.

In the present calculation, we obtain the proper ordering of the MO's as given by the *ab initio* calculations.[19] The calculated charge on Si is +3.40, which is higher than what we expect; this

TABLE IV. Energy levels (in eV) of $Si_2O$ molecular orbitals using various methods.[a]

| Bonding Nature | Reilly[b] (nonlinear $Si_2O$) | Abarenkov *et al.*[c] (nonlinear $Si_2O$) | Gilbert *et al.*[d] (collinear $Si_2O$) | Present calc. (collinear $Si_2O$)[e] | Present calc. (Nonlinear $Si_2O$) | Orbital composition |
|---|---|---|---|---|---|---|
| Nonbonding O 2$p$ Orbitals | −26.46 | −26.46 | −26.46 | −26.46 | −26.46 | 100% O 2$p$ |
| Bonding O 2$p$ Orbital | −28.16 | −26.46 | −26.46 | −26.46 | −26.56 | 100% O 2$p$ |
| Bonding O 2$s$ Orbital | −37.46 | −31.56 | −32.48 | −29.94 | −30.20 | 64% O 2$p$, 15% Si 3$s$, 21% Si 3$p$ |
| | −48.96 | −48.36 | −48.01 | −44.15 | −44.15 | 93% O 2$s$, 3% Si 3$s$, 4% Si 3$p$ |

[a] For comparison, the energy levels obtained by Reilly, Abarenkov *et al.*, and Gilbert *et al.* have been shifted down by 10.46, 16.26, and 10.08 eV, respectively, so that all top levels are equal.

[b] Reference 22.

[c] Reference 23.

[d] Reference 20.

[e] The collinear $Si_2O$ cluster is extracted from a $\beta$-cristobalite lattice (Si-O distance = 3.0368 bohr).

TABLE V. Experimental and calculated energies and intensities of $OK\alpha$ spectrum in $SiO_2$.

| Structure of $OK\alpha$ spectrum | Gilbert *et al.* RO[a] | Gilbert *et al.* FO[b] | Present calc. | Experiment[c] |
|---|---|---|---|---|
| Position of principal peak (eV) | 525.7 | 544.8 | 547.02 | 526 |
| Separation between principal peak and satellite (eV) | 6.9 | 6.0 | 3.7 | 4.7 |
| Intensity ratio | 3.9/1 | 2.4/1 | 3.1/1 | ~4/1 |

[a] Relaxed-orbital approximation, Ref. 20.
[b] Frozen-orbital approximation, Ref. 20.
[c] Reference 15.

large value probably occurs because the Si-Si interaction was excluded in the single $SiO_4$-cluster calculation. A detailed MO energy-level diagram for the $SiO_4$ cluster is given in Fig. 4. This diagram may be used to interpret the Si $K\beta$ and Si $L_{2,3}$ x-ray emission spectra.

The assigned transitions in the Si $K\beta$ and Si $L_{2,3}$ spectra are shown in Fig. 4. The calculated and experimental energy structures of these spectra are given in Table VII. In general, our results are in good agreement with experiments. However, the transitions given in Fig. 4 and Table VII were assigned without intensity considerations. In fact, the calculated Si $L_{2,3}$ intensities are in poor agreement with experiment, although the energies are quite good. The poor intensities may be due to the neglect of Si $3d$ orbitals and orbital relaxation effects in our calculation[19] and to inaccuracies in the orbitals themselves.

It is interesting to note that the $K\beta'$ (O $2s$) line in the Si $K\beta$ spectrum, (the $3t_2 \rightarrow$ Si $1s$ transition), is almost entirely a vertical transition which comes from the small Si $3p$ admixture (about 4.7%), in contrast to Fischer's crossover-transition theory.[36] It is also noted that our calculation is quite similar to the calculation by Tossell[27] in the sense that both calculations involve no empirical parameters and/or quantities in evaluating the diagonal and off-diagonal matrix elements of the Fock operator. The results from these two calculations also compare well with each other. However, Tossell's calculation did not obtain the proper ordering of the $1t_1$ and $5t_2$ orbitals and of the $4t_2$ and $5a_1$ orbitals, as compared with the self-consistent-field (SCF) calculation[19] (the present calculation yielded the same MO orderings as those obtained by the SCF calculation); the correct ordering of these orbitals may be significant in explaining the optical and x-ray spectra.[36a]

## VII. CALCULATIONS ON LARGER CLUSTERS

We have performed calculations on the $Si_2O_7$, $Si_5O_4$, and $Si_8O_7$ clusters which are shown in Figs.

TABLE VI. MO results for $SiO_4$ cluster by various methods.[a] (Energy in eV.)

| MO symmetry[b] | Louisñathan and Gibbs[c] *sp* | Louisñathan and Gibbs[c] *spd* | Collins *et al.*[d] *sp* | Collins *et al.*[d] *spd* | Tossell[e] *sp* | Present calc. *sp* Perfect $SiO_4$ | Present calc. *sp* Distorted $SiO_4$ |
|---|---|---|---|---|---|---|---|
| $1t_1$ | −23.63 | −23.63 | −23.63 | −23.63 | −23.63 | −23.63 | −23.63 |
| $5t_2$ | −23.55 | −23.64 | −23.63 | −26.16 | −22.36 | −25.13 | −25.14 |
| $1e$ | −23.92 | −24.42 | −24.70 | −29.26 | −25.38 | −27.36 | −27.36 |
| $4t_2$ | −24.40 | −24.70 | −30.76 | −31.44 | −28.69 | −28.59 | −28.58 |
| $5a_1$ | −25.29 | −25.30 | −34.30 | −33.89 | −28.25 | −29.84 | −29.84 |
| $3t_2$ | −40.77 | −40.99 | −55.79 | −57.36 | −46.62 | −43.43 | −43.42 |
| $4a_1$ | −42.97 | −42.98 | −56.99 | −58.32 | −48.48 | −46.29 | −46.29 |

[a] For comparison, the energy levels obtained by Louisñathan and Gibbs, Collins *et al.*, and Tossell have been shifted down by 8.02, 8.03, 50.84, 44.17, and 51.57 eV, respectively, so that all $1t_1$ levels are equal.
[b] Same notation was used as in Ref. 19.
[c] Reference 26.
[d] Reference 19.
[e] Reference 27.

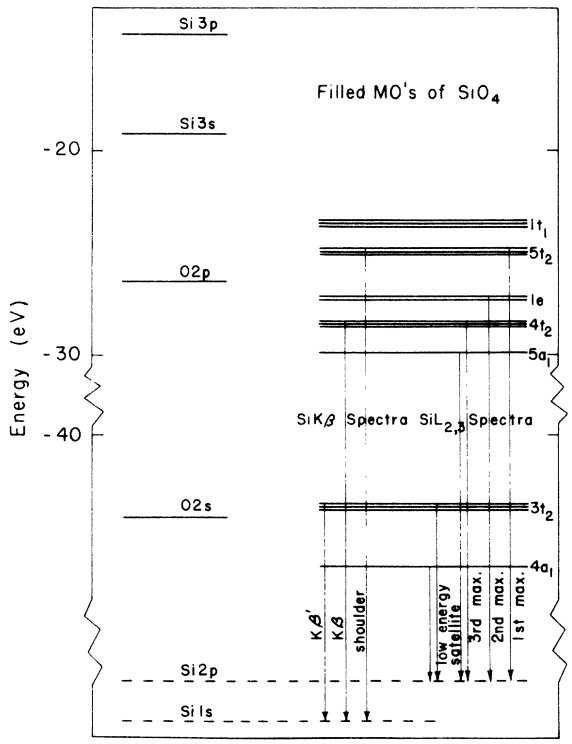


FIG. 4. MO energy-level diagram for $SiO_4$.

2(c), 2(d), and 1, respectively. Molecular energy levels for $Si_5O_4$, $Si_2O_7$, and $Si_8O_7$ are given in Fig. 5 (those for $SiO_4$ are also included for comparison). The orbital structures of these larger clusters were found to have the same basic features as those of the $Si_2O$ and $SiO_4$ clusters, namely, the valence orbitals consist of nonbonding O $2p$ orbitals at the top and bonding O $2p$ orbitals at the bottom of the band; and the O $2s$ band is at about 11 eV below the valence band.

It has been shown by Klein and Chun[15] that qualitative information about the densities of states in $SiO_2$ can be obtained from its x-ray spectra by assuming that maxima and shoulders in the x-ray spectra correspond to maxima in the densities of states in the crystal. Using the method of Klein and Chun, we redraw the x-ray-emission spectra of $SiO_2$ in Figs. 6(a), 6(b), and 6(c), in such a way that they have the same energy scale and only the peak positions of the spectra are given. The energy structure of the valence band of $SiO_2$ can then be obtained by combining these spectra together as shown in Fig. 6(d). Similarly, from the photoemission spectra of $SiO_2$ measured by DiStefano and Eastman,[16] we can construct the corresponding valence-band structure of $SiO_2$, as given in Fig. 6(e).

In order to compare the calculated valence-band structure for the $Si_2O_7$ cluster [Fig. 6(f)], as an example, with those determined from x-ray and photoemission spectra of $SiO_2$, the three valence bands have been brought together as shown in Fig. 6, by assuming that the Si $K\beta'$ emission corresponds to the lower-lying oxygen $2s^2$ level and the two upper overlapping peaks in the photoemission spectra correspond to the calculated two nonbonding oxygen $2p$ orbitals for the $Si_2O_7$ cluster. It can be seen that the calculated valence structure for the $Si_2O_7$ cluster is in good agreement with those determined from experiments. They all show a wide valence band (~9 eV) which is split into two groups corresponding to bonding and nonbonding O $2p$ orbitals.

In Table VIII, we summarize some other results from our cluster calculations for $SiO_2$.

TABLE VII. Experimental and calculated energy structures and intensities of the Si $K\beta$ and Si $L_{2,3}$ spectra in $SiO_2$.

| Structure of Si $K\beta$ spectra[a] | Assigned Transition | Collins *et al.*[b] ($SiO_4$;$spd$) $E$ (eV) | $\Delta E$ (eV) | Present calculation (distorted $SiO_4$;$sp$) $E$ | $\Delta E$ | $I$ | Experimental data[c] $E$ | $\Delta E$ | $I$ |
|---|---|---|---|---|---|---|---|---|---|
| Shoulder | $5t_2 \rightarrow$ Si 1s | 1836.64 | 5.28 | 1852.59 | 3.44 | 38 | 1835.0 | 3.3 | ~1-5 |
| $K\beta$ | $4t_2 \rightarrow$ Si 1s | 1831.36 | 0 | 1849.15 | 0 | 100 | 1831.7 | 0 | 100 |
| $K\beta'$ | $3t_2 \rightarrow$ Si 1s | 1805.44 | −25.92 | 1834.31 | −14.84 | 19 | 1818.0 | −13.7 | 15-20 |
| Structure of Si $L_{2,3}$ Spectra[d] | | | | | | | | | |
| 1st max. | $5t_2 \rightarrow$ Si 2p | 99.61 | 0 | 94.47 | 0 | ~0 | 94.5 | 0 | ~90 |
| 2nd max. | $1e \rightarrow$ Si 2p | 96.49 | −3.12 | 92.25 | −2.22 | | 92.3 | −2.2 | |
| 3rd max. | $5a_1, 4t_2 \rightarrow$ Si 2p | 91.88, 94.33 | −7.73, −5.28 | 89.77, 91.03 | −4.70, −3.44 | 100 | 89.0 | −5.5 | 100 |
| Low-energy satellite | $4a_1, 3t_2 \rightarrow$ Si 2p | 67.44, 68.41 | −32.17, −31.20 | 73.32, 76.19 | −21.15, −18.28 | 14 | 76.0 | −18.5 | 20-25 |

[a] For Si $K\beta$, $\Delta E$'s are given relative to $K\beta$.
[b] Reference 19.
[c] References 6, 9, and 27.
[d] For Si $L_{2,3}$, $\Delta E$'s are given relative to the 1st max.

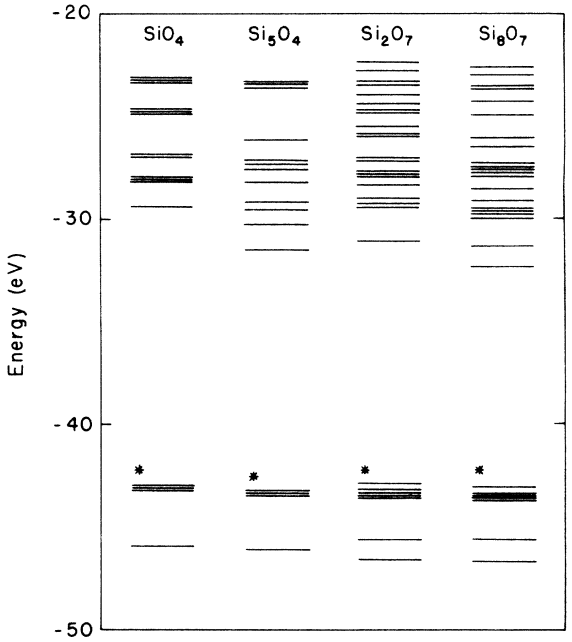


FIG. 5. Filled MO's for different clusters of $\alpha$-quartz.

(i) In all calculations, the charge on oxygen is about $-1.2$, which is fairly consistent with the assumed ionicity of oxygen. No effort was expended to obtain complete consistency because a large amount of computer time would have been required. This result indicates that the nature of the Si-O bonding in $SiO_2$ is neither purely ionic nor purely covalent, but is partly ionic and partly covalent.

(ii) In contrast with the results by Reilly[22] and Urch,[24] who obtained a large mixing of O $2s$ and O $2p$ orbitals, the oxygen $sp$ hybridization is quite small. For example, the atomic population of the bonding O $2s$ level ($Si_2O$) is 92.57% O $2s$, 0.00% O $2p$, 3.46% Si $3s$, and 3.97% Si $3p$.

(iii) For the larger clusters, the calculated valence-band widths are of the order of 9 eV, in good agreement with experimental values.

(iv) It is interesting to compare the calculated Wolfsberg-Helmholtz (WH) parameters $K_{\alpha\beta}$, which are defined by the WH approximation[37] $K_{\alpha\beta}=2F_{\alpha\beta}/S_{\alpha\beta}(F_{\alpha\alpha}+F_{\beta\beta})$, with the most often chosen value 1.75 in extended Hückel (EH) calculations.[38] The calculated $K_{\alpha\beta}$ between oxygen and oxygen (1.59 $\rightarrow$ 1.81), and between oxygen and silicon (1.55

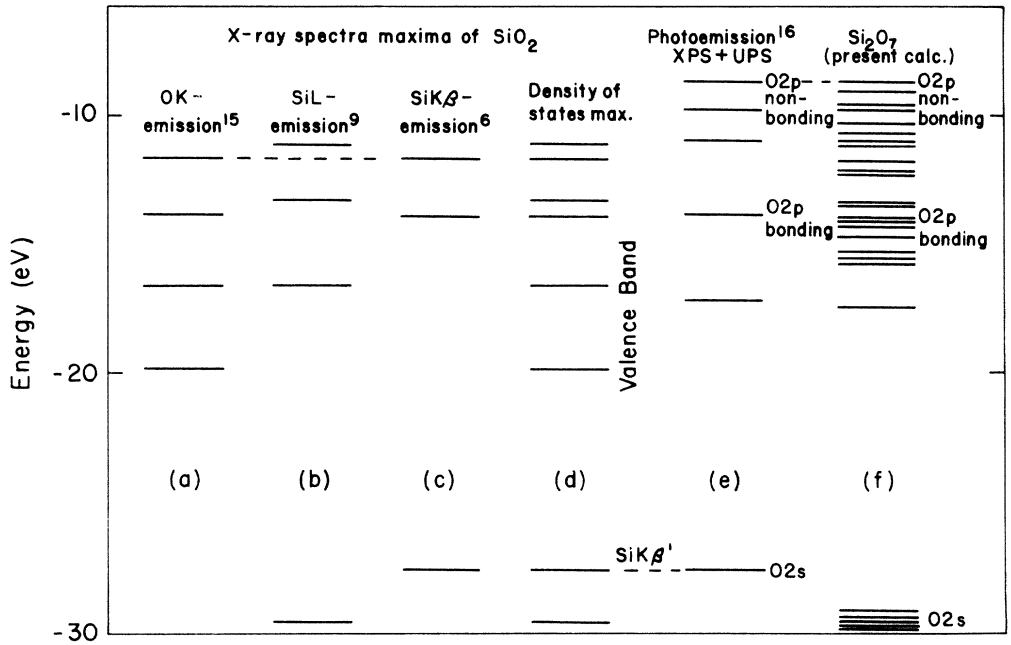


FIG. 6. Comparison of the calculated and experimental valence-band structures of $SiO_2$. (a) Oxygen $K$-emission spectral peaks (Ref. 15). (b) Silicon $L$-emission spectral peaks (Ref. 9). (c) Silicon $K\beta$-emission spectral peaks (Ref. 6). (d) Superposition of (a), (b), (c). (e) Photoemission spectral peaks (Ref. 16). (f) Calculated MO levels for $Si_2O_7$. The Si $K$- and $L$-emission spectra were brought to a common energy scale using the value 1740.3 eV for the Si $K\alpha_{1,2}$ doublet. The position of the O $K$-emission spectrum was assigned by the assumption that the maximum at 526.0 eV in the O $K$ spectrum and the shoulder at 1834.5 eV in the Si $K\beta$ spectrum are both due to transitions from the same valence-band levels. The common energy scale has its zero point at the bottom of the conduction band which we assume to be identical with the position of the Si $L$-absorption edge (see Ref. 15). The position of (e) was assigned by assuming that the Si $K\beta'$ band corresponds to the O $2s$ level. Spectra (e) and (f) can be compared with each other by assuming that the two upper overlapping peaks in the photoemission spectra correspond to the calculated two nonbonding oxygen $2p$ orbitals.

TABLE VIII. Summary of results for various cluster calculations.

| Other results | $Si_2O$ | $Si_2O_7$ | $Si_8O_7$ | $SiO_4$ | $Si_5O_4$ |
|---|---|---|---|---|---|
| Charge of central atom in cluster | −1.1849 (O) | −1.2830 (O) | −1.2018 (O) | +3.3960 (Si) | +2.7526 (Si) |
| Average charge of other atoms with saturated bonds in cluster | | +3.2474 (Si) | +2.7255 (Si)<br>−1.2320 (O) | | −1.1914 (O) |
| Oxygen $sp$ hybridization, e.g., orbital composition of the molecular orbital labeled by a star (*) in the MO energy-level diagrams (Figs. 3 and 5). | 92.57% 2$s$ (O)<br>0.0% 2$p$ (O)<br>3.46% 3$s$ (Si)<br>3.97% 3$p$ (Si) | 91.87<br>1.65<br>0.0<br>6.48 | 90.19<br>2.2<br>1.02<br>6.59 | 93.78<br>1.27<br>0.02<br>4.93 | 91.24<br>1.69<br>2.28<br>4.79 |
| Valence-band width (eV) | 3.7 | 8.7 | 9.8 | 6.2 | 8.2 |
| WH parameters $K_{\alpha\beta}=\frac{2F_{\alpha\beta}}{S_{\alpha\beta}(F_{\alpha\alpha}+F_{\beta\beta})}$ | Between O and O: $K_{\alpha\beta}=1.59\rightarrow 1.81$<br>O and Si: $1.55\rightarrow 1.66$<br>Si and Si: $0.57\rightarrow 0.85$ | | | | |

Crossover transitions, in a literal sense, are negligible.

→1.66) are not too far from 1.75, but those between silicon and silicon (0.57→0.85) are considerably smaller. This relatively weak Si-Si coupling is assumed to be responsible for the highly asymmetrical relaxation of the two silicon atoms neighboring the $O^-$ vacancy in the $E_1'$ center.[29] We shall discuss this type of relaxation effect in more detail in a separate paper.

(v) Crossover transitions in a literal sense are negligible. This result is consistent with the SCF calculations by Gilbert *et al.*[20]

## VIII. CONCLUSIONS

It has been shown that the present LCLO-MO cluster calculations have produced rather clear ideas about the nature of the valence states in $SiO_2$. However, the nature of the conduction states is not very well understood. There are two feasible refinements which can be made in order to obtain a better picture of the conduction band, including the width of band gap and the interpretation of the optical absorption spectra involving exciton and interband transitions.

(i) The inclusion of more distant neighbors (i.e., to use a larger cluster) would lessen the importance of the spurious surface effect.

(ii) As it was pointed out by Bennett and Roth[25] that the conduction band of $SiO_2$ is dominated by Si 3$d$ levels, the extension of the basis set by including Si 3$d$ orbitals would give a better description of the conduction states. The modifications (mainly in the orbital compositions) of the valence levels would also improve the Si $L_{2,3}$ intensities.

Also, the use of Schlosser's generalization[39] of the Adams-Gilbert equation and Gilbert's KO (kinetic-energy overlap) approximation to open-shell polyatomic systems would produce more accurate results than do the present calculations.

Further numerical studies on other metal and nonmetal oxides, such as $Al_2O_3$ and $GeO_2$, and theoretical work to include those modifications mentioned above are suggested in order to establish and improve the present LCLO cluster method such that it can be generally applied to other complex solid systems including transition-metal oxides.

## ACKNOWLEDGMENTS

The authors wish to thank David Strome for the use of his data on atomic positions in right-handed $\alpha$-quartz. Many helpful discussions with Dr. K. Klier, Dr. F. J. Feigl, and Dr. C. E. Jones, P. Hutta and P. Schneider are gratefully acknowledged. We thank Dr. T. L. Gilbert for his useful comments.

*Research supported by the National Science Foundation, Grant No. GH-33759.

†Present address: Dept. of Physics, University of Illinois, Urbana, Ill. 61801.

[1]K. L. Yip and W. B. Fowler, Phys. Rev. B 10, 1391 (1974), preceding paper.

[2]E. Loh, Solid State Commun. 2, 269 (1964).

[3]H. R. Phillipp, Solid State Commun. 4, 73 (1966).

[4]K. Platzöder, Phys. Status Solidi 29, K63 (1968).
[5]L. Pajasóva, Czech. J. Phys. B 19, 1265 (1969).
[6]D. W. Fischer, J. Chem. Phys. 42, 3814 (1965).
[7]W. L. Baun and D. W. Fischer, Spectrochimica Acta 21, 1471 (1965).
[8]R. A. Mattson and R. C. Ehlert, Adv. X-ray Anal. 9, 471 (1966).
[9]O. A. Ershov, D. A. Goganov, and A. P. Lukirskii, Fiz. Tverd. Tela 7, 2355 (1965) [Sov. Phys.–Solid State 7, 1903 (1966)]; R. J. Powell and G. Derbenwick, IEEE Trans. Nucl. Sci. NS18, 99 (1971).
[10]O. A. Ershov and A. P. Lukirskii, Fiz. Tverd. Tela 8, 2137 (1966) [Sov. Phys.–Solid State 8, 1699 (1967)].
[11]D. W. Fischer and W. L. Baun, Norelco Rept., 14, 92 (1967).
[12]G. Wiech, in *Soft X-Ray Band Spectra and the Electronic Structure of Metals and Materials*, edited by D. J. Fabian (Academic, New York, 1968), p. 59.
[13]C. G. Dodd and G. L. Glen, J. Applied Phys. 39, 5377 (1968); Am. Mineral. 54, 1299 (1969) [errata, *ibid.* 55, 1066 (1970)]; J. Am. Ceramic Soc. 53, 322 (1970).
[14]R. K. O'Nions and D. G. W. Smith, Nature (Phys. Sci.) 231, 130 (1971).
[15]G. Klein and H.-U. Chun, Phys. Status Solidi B 49, 167 (1972).
[16]T. H. DiStefano and D. E. Eastman, Phys. Rev. Lett. 27, 1560 (1971).
[17]T. H. DiStefano and D. E. Eastman, Solid State Commun. 9, 2259 (1971).
[18]R. W. G. Wyckoff, *Crystal Structures* (Interscience, New York, 1963), Vol. 1; R. L. Mozzi and B. E. Warren, J. Appl. Crystallogr. 2, 164 (1969).
[19]G. A. D. Collins, D. W. J. Cruickshank, and A. Breeze, J. Chem. Soc., Faraday Trans. II 68, 1189 (1972).
[20]T. L. Gilbert, W. J. Stevens, H. Schrenk, M. Yoshimine, and P. S. Bagus, Phys. Rev. B 8, 5977 (1973).
[21]A. R. Ruffa, Phys. Status Solidi 29, 605 (1968).
[22]M. H. Reilly, J. Phys. Chem. Solids 31, 1041 (1970).
[23]I. V. Abarenkov, A. V. Amosov, V. F. Bratsev, and D. M. Yudin, Phys. Status Solidi A 2, 865 (1970).
[24]D. S. Urch, J. Phys. C 3, 1275 (1970).
[25]A. J. Bennett and L. M. Roth, J. Phys. Chem. Solids. 32, 1251 (1971).
[26]S. J. Louisnathan and G. V. Gibbs, Am. Mineral 57, 1614 (1972).
[27]J. A. Tossell, J. Phys. Chem. Solids 34, 307 (1973).
[28]G. S. Smith and L. E. Alexander, Acta Crystallogr. 16, 462 (1963).
[29]F. J. Feigl, W. B. Fowler, and K. L. Yip, Solid State Commun. 14, 225 (1974).
[30]D. W. J. Cruickshank, J. Chem. Soc. 1077, 5486 (1961). A. G. Revesz, J. Non-Cryst. Solids 4, 347 (1970); Phys. Rev. Lett. 27, 1578 (1971).
[31]R. S. Mulliken, J. Chem. Phys. 23, 1833 (1955).
[32]The calculations of Madelung constants and point-ion potentials at the silicon and oxygen sites in $\beta$-cristobalite have been done by W. B. Fowler. He modified a computer program which was originally written by A. G. Piken and W. Van Gool (Chemistry Dept., Scientific Research Staff, Ford Motor Co.) to calculate the Madelung constants, and developed another computer program to calculate the point-ion potentials.
[33]C. C. J. Roothaan, Rev. Mod. Phys. 23, 69 (1951); 32, 179 (1960).
[34]R. E. Watson and A. J. Freeman, Phys. Rev. 123, 521 (1961).
[35]R. E. Watson, Phys. Rev. 111, 1108 (1958).
[36]D. W. Fischer, Adv. X-Ray Anal. 13, 159 (1970).
[36a]J. A. Tossell, D. J. Vaughan, and K. H. Johnson [Chem. Phys. Lett. 20, 329 (1973)] have published results on $(SiO_4)^{4-}$ using the $X_\alpha$ method. Our results agree with theirs in the ordering of energy levels, although actual values are somewhat different.
[37]M. Wolfsberg and L. Helmholtz, J. Chem. Phys. 20, 837 (1952).
[38]R. Hoffman, J. Chem. Phys. 39, 1397 (1963).
[39]H. Schlosser, J. Chem. Phys. 55, 5453 (1971); 5459 (1971).